

Evaluation of carbon isotope flux partitioning theory under simplified and controlled environmental conditions

Joel J. Fassbinder^{a,*}, Timothy J. Griffis^a, John M. Baker^{a,b}

^a Department of Soil, Water, and Climate, University of Minnesota, 439 Borlaug Hall, 1991 Upper Buford Circle, St. Paul, MN 55108, USA

^b USDA-ARS, Department of Soil, Water and Climate, University of Minnesota, St. Paul, MN, USA

ARTICLE INFO

Article history:

Received 27 November 2010

Received in revised form

22 September 2011

Accepted 26 September 2011

Keywords:

Stable carbon isotopes

Flux partitioning

Net ecosystem exchange

Automated chambers

Photosynthetic discrimination

Isotope composition of respiration

ABSTRACT

Separation of the photosynthetic (F_P) and respiratory (F_R) fluxes of net CO_2 exchange (F_N) remains a necessary step toward understanding the biological and physical controls on carbon cycling between the soil, biomass, and atmosphere. Despite recent advancements in stable carbon isotope partitioning methodology, several potential limitations can cause uncertainty in the partitioned results. Here, we combined an automated chamber system with a tunable diode laser (TDL) to evaluate carbon isotope partitioning under controlled environmental conditions. Experiments were conducted in a climate controlled greenhouse utilizing both soybean (C_3 pathway) and corn (C_4 pathway) treatments. Under these conditions, net exchange of $^{13}\text{CO}_2$ and $^{12}\text{CO}_2$ was obtained with an improved signal to noise ratio. Further, the chamber system was used to estimate soil evaporation (E) and plant transpiration (T), allowing for an improved estimate of the total conductance to CO_2 (g_c). This study found that the incorporation of short-term and diel variability in the isotope composition of respiration (δ_R) caused F_P to nearly double in the corn system while only slightly increasing in the soybean system. Variability in both g_c and the CO_2 bundle sheath leakage factor for C_4 plants (ϕ) also had a significant influence on F_P . In addition, chamber measurements of F_N and its isotope composition (δ_N) indicated that post-illumination processes caused a decrease in plant respiration for up to 3 h following light termination. Finally, this study found systematic differences between the isotope and temperature-regression partitioning methods on the diel time scale.

Published by Elsevier B.V.

1. Introduction

Measurement and analyses of carbon isotope fluxes have been used to partition ecosystem respiration (F_R) into its heterotrophic (F_{Rh}) and autotrophic (F_{Ra}) components (Rochette et al., 1999; Susfalk et al., 2002; Griffis et al., 2005; Millard et al., 2008), identify and quantify anthropogenic release of carbon into the atmosphere (Pataki et al., 2003b; Bush et al., 2007), and in particular, partition the net ecosystem exchange of CO_2 (F_N) into its photosynthetic (F_P) and respiratory (F_R) components (Yakir and Wang, 1996; Ogee et al., 2003; Bowling et al., 2003a; Zhang et al., 2006; Zobitz et al., 2007, 2008). Partitioning F_N into F_P and F_R remains a necessary step toward a deeper understanding of the biophysical controls on carbon cycling, which will ultimately lead to better constraint on the gross fluxes of F_P and F_R on the regional and global scales (see Table 1 for a summary of symbols).

Within the FLUXNET network (<http://www.fluxnet.ornl.gov>), F_N is traditionally partitioned into its respiratory and photosynthetic components by estimating either F_R from nighttime temperature

regression models or F_P from daytime light response curves (Goulden et al., 1996; Rustad et al., 2000; Falge et al., 2002; Griffis et al., 2003; Reichstein et al., 2005; Lasslop et al., 2010). Although widely used, these methods have several fundamental limitations. For nighttime temperature regression methods, limitations can include influences from variability in soil moisture (Davidson et al., 1998; Gaumont-Guay et al., 2006); transient response of soil respiration to rain events (Lee et al., 2004); an inability to capture short-term (diel) variability in F_N when using long-term (seasonal) temperature data (Reichstein et al., 2005); variation in the temperature sensitivity of soil respiration to changes in the size and turnover rate of labile carbon pools (Gu et al., 2004); and an inhibition of leaf respiration that occurs in the presence of light for several species, including corn (*Zea Mays*) (Kirschbaum and Farquhar, 1987; Atkin et al., 1997; Hurry et al., 2005). Further, the location of the soil temperature measurement has a significant influence on the Q_{10} value used in temperature regression partitioning and remains a major source of uncertainty (Mahecha et al., 2010). Estimates of F_P from light response models can be confounded by humidity and the location of the temperature measurement (i.e. above canopy, near surface, soil, etc.) which can alter temperature sensitivity calculations (Reichstein et al., 2005; Lasslop et al., 2010).

* Corresponding author.

E-mail address: fass0019@umn.edu (J.J. Fassbinder).

The stable isotope technique provides an independent approach to partitioning F_N into F_p and F_R . Yakir and Wang (1996) applied the mass balance principle to partition F_N using the unique carbon isotope signatures of the atmosphere, plants, and soil of an agricultural ecosystem. Their approach, however, was most effective over longer time scales because the isotope ratios assigned to the plants and soil were integrated values that did not account for short term variation in both the canopy-scale photosynthetic discrimination (Δ_{canopy}) and the carbon isotope composition of F_R (δ_R). Bowling et al. (2001) advanced the methodology of Yakir and Wang (1996) by combining eddy CO_2 flux measurements with $\delta^{13}C$ flask measurements (EC-flask isoflux partitioning method) to measure the net CO_2 isoflux ($F_N\delta_N$), over a deciduous forest. Further, their approach estimated Δ_{canopy} and allowed for short-term analysis of both F_N and F_R . Although this method allowed for high resolution measurement of F_N , measurement of δ_N was limited temporally due to the reliance on flask sampling and mass spectrometry.

Ogée et al. (2003) applied the EC-flask isoflux method to partition F_N by measuring the isotope flux profile within and above a coniferous forest. Further, a multilayer soil-vegetation-atmosphere transfer model (MuSICA) was utilized to estimate the total canopy conductance to CO_2 (g_c). Their study found that the MuSICA model was most effective during the daytime when isotope disequilibrium, defined as the difference between the isotope signatures of δ_R and photosynthesis (δ_p), was strong. In addition, their study emphasized the need for a reliable estimate of g_c and a better understanding of mesophyll conductance to CO_2 (g_m). Zobitz et al. (2008) demonstrated that although g_m directly influenced estimates of F_p and F_R using isotope partitioning, variability in g_m did not produce unrealistic partitioning results. Further, their study suggested that for ecosystem-scale experiments, leaf-level estimates of g_m need to be scaled up to the canopy-level.

Zhang et al. (2006) used carbon isotope flux partitioning over an agricultural ecosystem under C_3/C_4 crop rotation utilizing the flux-gradient method. Their study incorporated the added complexity of a C_4 ecosystem, which requires a slightly more complicated Δ_{canopy} calculation due to an additional step (PEP carboxylation) that occurs during C_4 photosynthesis (Farquhar, 1983). In addition, their study calculated the isotope signature of F_N using the flux-ratio approach rather than the traditional Keeling method (Keeling, 1958; Pataki et al., 2003a) and improved the temporal resolution of the flux-gradient measurement with the use of a tunable diode laser (TDL) absorption spectrometer. The flux-gradient method, however, generally showed high variability in δ_N and tended to give underestimated and sometimes unrealistic F_p values due to uncertainty associated with gradient measurement in a well-mixed surface layer (Griffis et al., 2005).

High resolution measurements of $^{13}CO_2$ and $^{12}CO_2$ were combined with a Bayesian optimization approach by Zobitz et al. (2007) to estimate the flux components of F_N in a subalpine forest. Their study determined that several limitations of the isotope method exist, including difficulty in obtaining an accurate estimation of the isoflux, which could not be directly measured at the time of the study. Also, their study determined that a small isotope disequilibrium limited the effectiveness of the carbon isotope partitioning method on the diel time scale.

Billmark and Griffis (2009) expanded on these previous works by combining eddy covariance and tunable diode laser (TDL) techniques to partition the component fluxes of F_N above a C_3 (soybean) ecosystem. The EC-TDL method allowed for the isoflux to be measured directly, eliminating the need for gradient measurement and allowing for a much higher resolution analysis of the net isotope exchange of carbon between the land and atmosphere. Their study concluded that within the C_3 ecosystem on the seasonal time scale, δ_R was strongly linked to the isotope discrimination associated with the photosynthetic pathway of the vegetation. This coupling was

found to impact isotope flux partitioning of F_N after peak growth when the isotope disequilibrium was small. Further, their study confirmed that uncertainty associated with the g_c calculation is a major challenge when partitioning the component fluxes of F_N on the ecosystem scale (Bowling et al., 2001).

Traditionally, g_c is calculated by inverting the Penman–Monteith equation (Bowling et al., 2001; Ogée et al., 2003; Zhang et al., 2006). This method, however, requires several independent environmental measures including temperature, vapor pressure deficit (VPD), and latent and sensible heat. Each additional measurement carries its own level of uncertainty and noise. When these variables are incorporated into the Penman–Monteith equation, the propagation of error can be significant, leading to uncertainty as high as 30% (Bowling et al., 2001; Zhang et al., 2006). Further, the Penman–Monteith equation includes the unknown contributions of surface and soil evaporation, which can lead to further uncertainty in the partitioned results. Knohl and Buchmann (2005) found that under wet conditions, canopy conductance was overestimated using the Penman–Monteith equation which produced erroneous Δ_{canopy} and F_p values.

One of the major assumptions in carbon isotope partitioning theory is that the isotope composition of respiration is constant over time. Several studies have suggested that δ_R can vary both on the seasonal and diel time scales. Griffis et al. (2005) showed that δ_R can vary by as much as 15‰ over the course of an agricultural growing season. Drewitt et al. (2009) observed a gradual decrease of 4‰ in the isotope composition of soil respiration (δ_{RS}) from an agricultural field after corn harvest due to the gradual decrease of microbial decomposition of fresh corn residue. Fassbinder et al. (2012) observed a 4‰ increase in δ_{RS} from early to peak growth during a corn growing season due to the increased contribution of both corn root respiration and microbial consumption of root exudates. Another factor influencing the variability in δ_R is post-photosynthetic isotope fractionation, which has been shown to occur during the accumulation and re-mobilization of assimilates throughout the plant (Gessler et al., 2008; Kodama et al., 2008; Barbour et al., 2011) and during dark respiration (Ghashghaie et al., 2001; Klumpp et al., 2005). These processes can cause the isotope signatures of above and below ground respiration to differ from the isotope signature of newly assimilated CO_2 , leading to uncertainty in the isotope signature of autotrophic respiration (δ_{Ra}). Significant variation in δ_R , caused by either changes in phenology, microbial carbon sources, or post-photosynthetic fractionation, can affect the isotope disequilibrium between δ_R and δ_p and can confound carbon isotope partitioning techniques (Bowling et al., 2008; Billmark and Griffis, 2009).

In C_4 ecosystems, application of the carbon isotope partitioning method requires the estimation of the bundle sheath leakage factor, ϕ . During C_4 photosynthesis, a fraction of CO_2 produced in the bundle sheath cells leaks into the mesophyll cells where it is refixed by rubisco (Evans et al., 1986; Farquhar et al., 1989). Values of ϕ generally range between 0.2 and 0.5 (Sun et al., 2010). Zhang et al. (2006) used an optimized ϕ value of 0.3 for a corn canopy, although they acknowledged that ϕ was unlikely to remain constant throughout the growing season and concluded that further investigation is needed on the factors causing variation in ϕ .

In this study, a simplified approach was taken to carbon isotope partitioning methodology by combining an automated chamber system with tunable diode laser (TDL) spectroscopy in a climate controlled greenhouse utilizing chamber plots with mixed C_3/C_4 soil and either soybean (C_3 pathway) or corn (C_4 pathway) plants. This chamber-TDL method is capable of continuous, direct measurement of both evapotranspiration (ET) and δ_N , eliminating the use of both the Penman–Monteith equation and the measurement of F_N utilizing eddy covariance or gradient techniques. Three

Table 1
Symbols used in the text.

| | |
|-------------------------------|--|
| a | Kinetic isotope fractionation associated with diffusion through the stomata, ‰ |
| b_3 | Enzymatic isotope fractionation associated with rubisco carboxylation, ‰ |
| b_4 | Enzymatic isotope fractionation associated with PEP carboxylase, ‰ |
| C_a | Atmospheric CO ₂ mole mixing ratio, $\mu\text{mol mol}^{-1}$ |
| C_c | CO ₂ mole mixing ratio at the site of carboxylation, $\mu\text{mol mol}^{-1}$ |
| CO ₂ | Total carbon dioxide mole mixing ratio including all isotopologues, $\mu\text{mol mol}^{-1}$ |
| ¹² CO ₂ | Carbon dioxide isotopologue (mass 44) mole mixing ratio, $\mu\text{mol mol}^{-1}$ |
| ¹³ CO ₂ | Carbon dioxide isotopologue (mass 45) mole mixing ratio, $\mu\text{mol mol}^{-1}$ |
| δ_a | Carbon isotope ratio of ambient air, ‰ |
| δ_N | Carbon isotope ratio of net CO ₂ exchange, ‰ |
| δ_P | Carbon isotope ratio of photosynthesis, ‰ |
| δ_R | Carbon isotope ratio of ecosystem respiration, ‰ |
| δ_{Ra} | Carbon isotope ratio of autotrophic respiration, ‰ |
| δ_{Rs} | Carbon isotope ratio of soil respiration, ‰ |
| δ_{SOM} | Carbon isotope ratio of soil organic matter, ‰ |
| Δ_{canopy} | Canopy-weighted photosynthetic discrimination, ‰ |
| E | Soil evaporation, $\text{mmol m}^{-2} \text{s}^{-1}$ |
| ET | Evapotranspiration, $\text{mmol m}^{-2} \text{s}^{-1}$ |
| F_N | Net ecosystem CO ₂ exchange, $\mu\text{mol m}^{-2} \text{s}^{-1}$ |
| F_P | Net ecosystem photosynthesis, $\mu\text{mol m}^{-2} \text{s}^{-1}$ |
| F_R | Nonfoliar ecosystem respiration, $\mu\text{mol m}^{-2} \text{s}^{-1}$ |
| F_{Ra} | Autotrophic respiration, $\mu\text{mol m}^{-2} \text{s}^{-1}$ |
| F_{Rh} | Heterotrophic respiration, $\mu\text{mol m}^{-2} \text{s}^{-1}$ |
| F_{TER} | Total ecosystem respiration, $\mu\text{mol m}^{-2} \text{s}^{-1}$ |
| F_L | Foliar ecosystem respiration, $\mu\text{mol m}^{-2} \text{s}^{-1}$ |
| $F_N\delta_N$ | Net CO ₂ isoflux, $\mu\text{mol m}^{-2} \text{s}^{-1} \text{‰}$ |
| g_a | Aerodynamic conductance to CO ₂ , $\text{mol m}^{-2} \text{s}^{-1}$ |
| g_b | Boundary layer conductance to CO ₂ , $\text{mol m}^{-2} \text{s}^{-1}$ |
| g_c | Canopy conductance to CO ₂ , $\text{mol m}^{-2} \text{s}^{-1}$ |
| g_m | Mesophyll conductance to CO ₂ , $\text{mol m}^{-2} \text{s}^{-1}$ |
| g_s | Stomatal conductance to CO ₂ , $\text{mol m}^{-2} \text{s}^{-1}$ |
| g_w | Stomatal conductance to water vapor, $\text{mol m}^{-2} \text{s}^{-1}$ |
| ϕ | CO ₂ leakage factor in the bundle sheath, dimensionless |
| T | Transpiration, $\text{mmol m}^{-2} \text{s}^{-1}$ |
| TDL | Tunable diode laser |
| w_a | Mole mixing ratio of water vapor inside the chamber headspace, mmol mol^{-1} |
| w_i | Mole mixing ratio of water vapor inside of the leaf, mmol mol^{-1} |

fundamental questions pertaining to isotope partitioning theory were explored. First, can partitioning results with low uncertainty be obtained if the signal to noise ratios of g_c and the isoflux are improved? Second, how do both short-term and long-term variability in δ_R affect partitioned results? Third, are there systematic differences between the isotope and temperature-regression partitioning methods? To answer these questions, this study (1) utilized the carbon isotope partitioning method to estimate F_R and F_P from corn and soybean chambers in a climate controlled greenhouse, (2) partitioned F_N from the corn and soybean chambers using nighttime temperature response techniques and compared results with the isotope method, and (3) evaluated C₃ and C₄ isotope partitioning theory and identified potential challenges and problems.

2. Materials and methods

2.1. Plant growth facility

Laboratory measurements were conducted at the University of Minnesota Plant Growth Facilities, located on the St. Paul campus. A combination of electric heaters, overhead vents, and exhaust fans controlled the greenhouse temperature within a range of 2 °C of the set point. Lighting was supplied by forty 800 W sodium halide bulbs evenly spaced throughout the greenhouse and controlled by an Argus Control System (Argus Controls, Controller Model 100, White Rock, British Columbia, Canada).

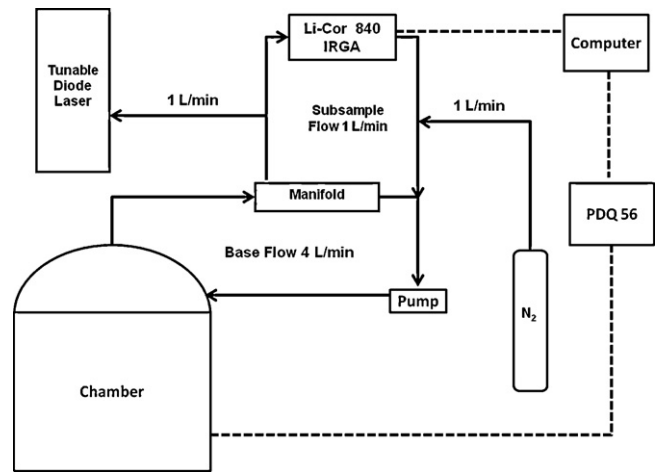


Fig. 1. Schematic of the automated chamber system and TDL for isotope analysis.

2.2. Chamber and tunable diode laser system

A closed, non-steady state chamber system was used for a 25 day period to measure carbon isotope fluxes and evapotranspiration. The chamber system used for this study was designed by the Biometeorology and Soil Physics Group at the University of British Columbia and consisted of fully automated, flow through chambers capable of measuring fluxes of water vapor and CO₂ (Gaumont-Guay et al., 2006). Each chamber lid was made of clear acrylic and had a headspace volume of 0.06 m³.

Chamber lids were closed using compressed air supplied by an electric air compressor (Powermate, Model VPP0301104, Long Grove, IL). Closure of the chamber lids was controlled by a 12 Vdc solenoid valve mounted to the back of each chamber. Upon closure, a small fan inside the chamber headspace was activated to ensure air was well mixed during sampling. A portable data acquisition module (Iotech PDQ56, Cleveland, OH, USA) and a personal computer were used to record all chamber signals including CO₂ and water vapor concentrations as well as thermocouples. All calculations and data processing were performed using custom software developed in Matlab (The Mathworks Inc., Natick, MA, USA).

Synflex tubing (Synflex Type 1300, Aurora, OH, USA) carried air from the sample inlet to a custom made manifold that controlled sampling to a Li-Cor 840 IRGA (Li-Cor Inc., Lincoln, NE, USA). After air from the sample line was analyzed by the IRGA, a diaphragm pump (Model NMP850KNDCB, KNF Neuberger Inc., Trenton, NJ, USA) returned the air back to the chamber headspace in a separate Synflex tube (return line) (Fig. 1). The base flow rate through the chamber system was set at 4 L min⁻¹ with a subsample flow through the IRGA set at 1 L min⁻¹. Sampling frequency and length of individual sampling events were set to 15 min and 210 s, respectively. The individual sampling time was optimized to accurately measure the rate of isotope mixing ratio change inside the chamber while minimizing chamber artifacts that can adversely impact the flux (Wagner et al., 1997).

Each chamber was fitted to a 200 L PVC soil column (53 cm diameter, 91 cm height) that was sealed at the bottom. Approximately 260 kg of soil from the Rosemount Research and Outreach Center (RROC) was added to each column. The soil is a Waukegan silt loam with a relatively high organic carbon content (2.6%) (Baker and Griffis, 2005). The average isotope composition of the soil organic matter (δ_{SOM}) is -18‰ in the 0–40 cm soil layer with values between -15 and -13‰ observed in deeper layers (Griffis et al., 2005). The soil was extracted from the agricultural field site where previous work was conducted by Baker and Griffis (2005), Zhang et al. (2006), Griffis et al. (2008), Billmark and Griffis (2009). The

soil profile at RROC was replicated inside each column in order to maintain continuity between the field and greenhouse. However, we acknowledge that some disturbance of the soil matrix was unavoidable and likely caused changes in the bulk density, soil water content, and tortuosity values of the soil column that may impact the processes being studied.

The experiment utilized three automated soil chambers. Two of the chambers contained either corn or soybean plants while the third chamber was left as a bare soil control. Each treatment chamber had 60 evenly spaced seeds sown at a depth of 2–5 cm. Due to the limited space available in the chamber headspace, vegetation was not allowed to reach a mature stage. This restriction limited the focus of the experiment to partitioning F_N into F_P and F_R during early plant growth. Continuous sampling of F_N , δ_N , soil and air temperature, and soil water content was performed for a 25 day period in the greenhouse. The diel greenhouse temperature was set to a daytime high of 28 °C and a nighttime low of 17 °C. Greenhouse lighting was turned on from 0600 to 2000 h daily. Watering was performed every three to four days and averaged about 9.5 mm of water per watering event per chamber.

Soil temperature was measured at depths of 5, 10, and 30 cm as well as at 10 cm above the surface using chromel-constantan thermocouples. Half hourly volumetric soil water content was also measured for two of the chambers using Em50 ECH₂O sensors (Decagon Devices, Inc., Pullman, WA, USA) at depths of 10 and 20 cm.

2.3. Carbon isotope partitioning: theory and measurement

Based on the mass balance principle, F_N , F_P , and F_R , as well as their carbon isotope signatures, can be written after Bowling et al. (2001) as

$$F_N = F_R + F_P \quad (1)$$

$$\delta_N F_N = \delta_R F_R + (\delta_a - \Delta_{canopy}) F_P \quad (2)$$

where δ_a is the carbon isotope ratio of ambient air, Δ_{canopy} is the whole canopy photosynthetic discrimination, and δ_N is the isotope ratio of F_N . Nonfoliar ecosystem respiration (F_R) is defined as $F_R = F_{TER} - F_L$, where F_{TER} is total ecosystem respiration and F_L is foliar respiration (Farquhar and Sharkey, 1982; Zobitz et al., 2007; Griffis et al., 2008). Sign convention for this study defines a positive flux leaving the surface and a negative flux directed toward the surface. The δ_R term, equal to the isotope composition of nighttime F_R , is assumed to have no diel variation (Zhang et al., 2006; Zobitz et al., 2007). For this study, δ_R was set at -17 and -23‰ for the corn and soybean chambers, respectively. These values are equal to the average nightly δ_R measurement observed during the last 15 days of the experiment.

Assuming that leaf-level and chamber-level photosynthesis are analogous (chamber-level considered a “big leaf”), F_P is estimated using (Farquhar et al., 1989; Bowling et al., 2001)

$$-F_P = g_c(C_c - C_a) \quad (3)$$

where g_c is the total conductance to CO₂ (mol m⁻² s⁻¹), C_c is the CO₂ mole mixing ratio at the site of carboxylation (μmol mol⁻¹), and C_a is the atmospheric CO₂ mole mixing ratio. Here, C_a was measured directly and C_c was solved for.

Values of g_c were derived from

$$\frac{1}{g_c} = \frac{1}{g_s} + \frac{1}{g_m} \quad (4)$$

where g_s and g_m are the stomatal and mesophyll conductances to CO₂, respectively. Previous partitioning studies have also included the terms for the aerodynamic (g_a) and boundary layer (g_b) conductances to CO₂ (Ogée et al., 2003; Zhang et al., 2006; Zobitz

et al., 2007; Billmark and Griffis, 2009). However, in this study we used the chamber water vapor fluxes to estimate g_s based on mass balance (Kim and Lee, 2011). Therefore, g_a and g_b were not measured directly. We have assumed that in a well-ventilated growth chamber $1/g_a$ and $1/g_b$ are very small relative to $1/g_s$, so that total conductance to CO₂ is reasonably constrained (see calculations below). Values of g_m were set at 0.87 and 0.40 mol m⁻² s⁻¹ for the corn and soybean chambers, respectively, based on literature values (Billmark and Griffis, 2009).

Soil evaporation (E) and evapotranspiration (ET) were measured using

$$F = \frac{P \cdot V \cdot dw_a/dt}{A \cdot T_a \cdot R} \quad (5)$$

where F represents either E or ET, dw_a/dt is the change in water vapor mixing ratio over time (mmol mol⁻¹ s⁻¹), P is atmospheric pressure (98 500 Pa), V is the volume of the chamber, A is the surface area of the chamber (0.216 m²), T_{air} is the chamber air temperature (K), and R is the gas constant (8.3144 m³ Pa K⁻¹ mol⁻¹). Due to the rapidly changing environmental conditions inside the chamber after closure, dH_2O/dt was calculated using linear regression and only included data from the first 15 s of the sampling event after an initial omit time of 15 s following chamber closure. Linear regressions with an r^2 coefficient less than 0.95 were excluded from the analysis.

Transpiration (T) was separated from ET using

$$T = ET - E \quad (6)$$

where E is the water vapor flux from a bare soil control chamber.

Total conductance to H₂O (g_w) was calculated using

$$T = g_w(w_i - w_a) \quad (7)$$

with w_i and w_a the mole mixing ratios (mmol mol⁻¹) of water vapor inside of the leaf and in the chamber headspace, respectively (Cowan and Farquhar, 1977). The mole mixing ratio w_i was taken to be the saturated mixing ratio at the leaf temperature. The water vapor mixing ratio in the chamber headspace (w_a) was defined as the mixing ratio at the time of chamber closure. The bulk stomatal conductance to CO₂ (g_s) was then calculated by applying the ratio of the diffusivities of H₂O to CO₂ in the air (≈ 1.6) to g_w (Farquhar and Sharkey, 1982). There are three sources of uncertainty associated with the g_s calculation. First, the g_a and g_b terms were not explicitly accounted for in the g_w calculation (Kim and Lee, 2011), causing a slight overestimation of g_s . Second, the rapidly changing environmental conditions inside of the chamber shortly after closure may have caused an underestimate of E and ET. Third, due to a lack of plant shade, values of E from the control chamber may have been slightly higher than E in the planted chambers and caused a slight underestimate of T .

For a C₃ ecosystem, Δ_{canopy} can be calculated using Farquhar et al. (1989)

$$\Delta_{canopy} = a + (b_3 - a) \frac{C_c}{C_a} \quad (8)$$

where a represents the kinetic isotope fractionation associated with diffusion through the stomata (4.4‰) and b_3 represents the enzymatic isotope fractionation associated with ribulose 1,5 bisphosphate carboxylase/oxygenase (rubisco) carboxylation (29‰) during the Calvin Cycle.

Isotope partitioning in a C₄ ecosystem is more complex due to the carboxylation of phosphoenolpyruvate (PEP) in the mesophyll cells. This process forms a C₄ acid such as malate or aspartate which is transported to the bundle sheath cells where it is decarboxylated. CO₂ that is generated in the bundle sheath cells during decarboxylation is then reduced to carbohydrates via the Calvin cycle (Taiz and Zeiger, 2002). The Δ_{canopy} value for a C₄ ecosystem must account for

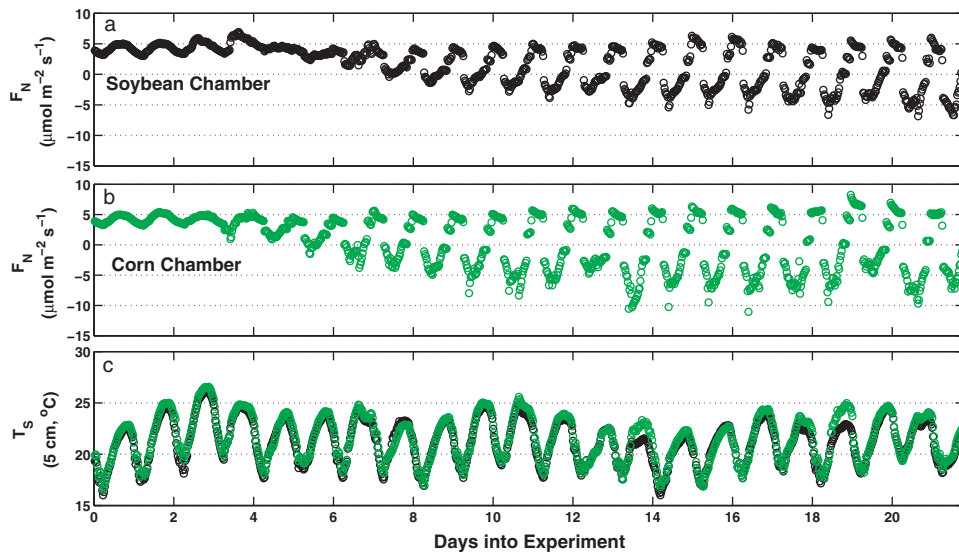


Fig. 2. Half-hourly measurements of F_N from the (a) soybean (black symbols) and (b) corn (green symbols) chambers, and (c) half-hourly measurements of soil temperature at the 5 cm depth for both chambers. (For interpretation of the references to color in this figure legend, the reader is referred to the web version of the article.)

the fraction of CO_2 produced in the bundle sheath cells that leaks into the mesophyll cells (ϕ) (Farquhar, 1983),

$$\Delta_{\text{canopy}} = a + (b_4 + b_3\phi - a) \frac{C_c}{C_a} \quad (9)$$

where b_4 is the isotope fractionation associated with PEP carboxylase (-5.7%) (Farquhar et al., 1989; Zhang et al., 2006). The value of ϕ , usually between 0.2 and 0.5, has a direct influence on Δ_{canopy} . In our study, ϕ was optimized by initially being set at 0.2 and increased/decreased incrementally by 0.02 until nighttime F_P adjusted to zero. Using this criterion, ϕ was estimated as 0.46. By combining Eqs. (2) and (3) with either Eq. (4) or (5) (depending on the photosynthetic pathway), F_P can be obtained from the analytical solution of this non-linear set of equations (Bowling et al., 2001; Zobitz et al., 2008; Billmark and Griffis, 2009).

2.3.1. Net CO_2 exchange and its carbon isotope ratio

Measurement of F_N within each chamber was calculated using

$$F_N^x = \frac{P \cdot V \cdot d^x \text{CO}_2 / dt}{A \cdot T_{\text{air}} \cdot R} \quad (10)$$

where the superscript x indicates either the isotopologue $^{12}\text{CO}_2$ or $^{13}\text{CO}_2$. A best fit linear regression was used to determine dc/dt for each sampling event. Linear regressions with an r^2 coefficient less than 0.95 were excluded from the analysis. For each chamber measurement the first 15 s were omitted from each sampling event to eliminate potential perturbation from lid closure, leaving the remaining 195 s of the chamber sample to calculate the slope. The isotope composition of F_N was determined from the flux ratio, F^{13}/F^{12} , and was expressed in delta notation using

$$\delta_N = \left(\frac{F^{13}/F^{12}}{R_{\text{VPBD}}} - 1 \right) \times 1000 \quad (11)$$

2.3.2. Tunable diode laser system

The stable isotopologues $^{12}\text{CO}_2$ and $^{13}\text{CO}_2$ were measured using tunable diode laser (TDL) spectroscopy (TGA100, Campbell Scientific, Logan, UT, USA) (Bowling et al., 2003b; Griffis et al., 2004, 2005). Air flow from the chamber system to the TDL was set at $7.44 \times 10^{-4} \text{ mol s}^{-1}$ (1 L min^{-1}). The TDL used to measure the isotope composition of (δ_N) was housed in an adjacent greenhouse bay with a constant temperature of approximately 18°C to help maintain a stable operating temperature. Chamber air analyzed by

the TDL was not returned to the chamber. To compensate, N_2 gas flowing at $7.44 \times 10^{-4} \text{ mol s}^{-1}$ was added to the chamber return line. Replacement of air sampled by the TDL with N_2 gas caused a dilution of the chamber CO_2 concentration, resulting in an underestimate of the true flux. A correction factor was obtained from the product of the N_2 flow rate into the chamber and the mean chamber concentration of either $^{12}\text{CO}_2$ or $^{13}\text{CO}_2$ (Griffis et al., 2011). Using this method, the theoretical dilution flux was calculated at -1.17 and $-0.0138 \mu\text{mol m}^{-2} \text{ s}^{-1}$ for F^{12} and F^{13} , respectively. Applying this correction caused δ_N to increase by 0.4% . Also, the addition of N_2 gas likely diminished the amount of O_2 available for leaf respiration. However, due to the short sample time (210 s) and large chamber volume (60 L), the decrease in oxygen was small (from 20.95% to 19.90% at the end of sampling) and likely had a minimal influence on leaf respiration.

3. Results and discussion

3.1. Phenology of chamber vegetation

Prior to planting, soil respiration showed strong diel variability in all chambers, with a daytime high of about $6 \mu\text{mol m}^{-2} \text{ s}^{-1}$ and a nighttime low of about $3 \mu\text{mol m}^{-2} \text{ s}^{-1}$. After planting, the corn and soybean plants showed rapid phenological changes, with leaf emergence occurring 4 days after planting and within 15 days the corn and soybean plants had reached 25 cm, exceeding the height of the chamber lid. Before the corn and soybean plants interfered with chamber closure, daytime F_N reached $-7 \mu\text{mol m}^{-2} \text{ s}^{-1}$ in the soybean chamber and $-10 \mu\text{mol m}^{-2} \text{ s}^{-1}$ in the corn chamber (Fig. 2a and b). Every morning, photosynthetic CO_2 uptake was activated much more abruptly in the greenhouse than what is typically observed under field conditions due to the artificial light source. Light activation caused F_N to drop sharply at 0600 h from 6 to $-3 \mu\text{mol m}^{-2} \text{ s}^{-1}$ in the corn chamber and from 5 to $-1 \mu\text{mol m}^{-2} \text{ s}^{-1}$ in the soybean chamber. Net CO_2 exchange reached -7 and $-5 \mu\text{mol m}^{-2} \text{ s}^{-1}$ in the corn and soybean chambers, respectively, at 1000 h and gradually became less negative in both planted chambers throughout the afternoon. From 2300 to 0600 h, nighttime F_R gradually decreased in both planted chambers from about 6 to $4 \mu\text{mol m}^{-2} \text{ s}^{-1}$, with F_R from the corn chamber consistently 0.25 to $0.50 \mu\text{mol m}^{-2} \text{ s}^{-1}$ higher than F_R from the soybean chamber. In the bare soil control chamber, F_R showed a strong

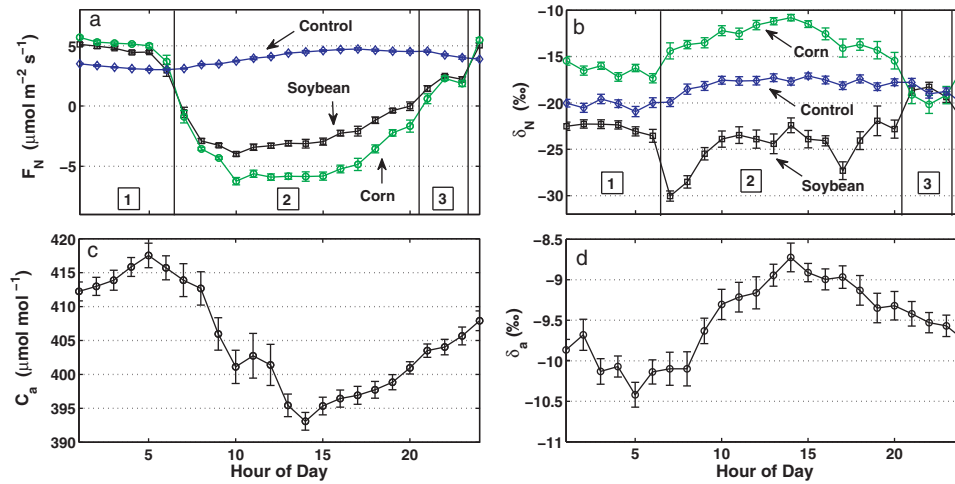


Fig. 3. Diel signal of (a) F_N , (b) δ_N for the corn (green circles), soybean (black squares), and bare soil (blue diamonds) chambers. Also plotted is the (c) ambient CO_2 concentration inside of the greenhouse and (d) the isotope ratio of ambient CO_2 concentration. Diel ensembles were created with data from the last 15 days of the experiment. In some cases, the standard error bars are smaller than the symbol used. Phases 1, 2, and 3 in panels a and b correspond to distinct physiological shifts in F_N and δ_N that were observed during the last 15 days of the experiment. (For interpretation of the references to color in this figure legend, the reader is referred to the web version of the article.)

diel pattern reaching a daytime maximum of $4.7 \mu\text{mol m}^{-2} \text{s}^{-1}$ at 1700 h and a nighttime minimum of $3.0 \mu\text{mol m}^{-2} \text{s}^{-1}$ at 0600 h just prior to light activation.

3.2. Carbon isotope composition of F_N and F_R

The strong diel pattern observed in δ_N suggests that there were three distinct phases related to F_N , including (1) late night/early morning mix of heterotrophic (F_{Rh}) and autotrophic (F_{Ra}) respiration, (2) daytime photosynthetic uptake, and (3) early evening inhibition of F_{Ra} shortly after light deactivation (Fig. 3a and b). In the corn chamber, daytime δ_N showed a strong C_4 signal at -11‰ due to photosynthetic discrimination. Soybean δ_N showed a C_3 signal at 1000 h at -29‰ but increased during the afternoon, reaching -19‰ at 2000 h. Values of δ_N were highly variable from 1800 to 2000 h when F_N was near zero. Nighttime values of δ_R (from 0000 to 0600 h) in the corn chamber averaged -16‰ , which is slightly enriched relative to δ_{SOM} and suggests that corn F_{Ra} contributed significantly to total F_R during this period. Nighttime values of δ_R averaged -22‰ in the soybean chamber, indicating a strong contribution from soybean F_{Ra} . In the bare soil control chamber, the isotope composition of soil respiration (δ_{RS}) showed a diel pattern consisting of daytime enrichment followed by a gradual depletion after light termination. Total diel variation in δ_R was about 3‰ , reaching -17‰ during the afternoon and -20‰ during the nighttime. The diel δ_R pattern observed in the control chamber may have been due to a soil temperature gradient, which caused varying contributions from deeper, isotopically heavier soil layers (Fassbinder et al., 2012).

Immediately after the lights were turned off at 2000 h (when $F_N = F_R$), δ_R sharply decreased in the corn chamber from -16‰ to -19‰ (Phase 3, Fig. 3a and b). The δ_R signal remained at this value until 0100 h, at which time it increased to -16‰ and remained near this value until the lighting was reactivated at 0600 h. In the soybean chamber, δ_R sharply increased from -23 to -19‰ immediately after light termination and remained at this value until 0000 h. At this time, δ_R in the soybean chamber decreased to -22‰ and remained near this value until the lighting was reactivated at 0600 h. Chamber-TDL data show that values of F_R and δ_R from the planted chambers were similar to values in the bare soil control chamber, suggesting that autotrophic respiration (F_{Ra}) was diminished during this 3 h period (2100 to 0000 h). Respiration rates were

$2\text{--}3 \mu\text{mol m}^{-2} \text{s}^{-1}$ lower during this 3 h period than nighttime F_R values when autotrophic respiration was a strong contributor. It should also be noted that the termination of greenhouse lighting (2000 h) occurred about 2 h after the average time of sunset (1800 h), meaning that F_N was not influenced by natural light during this 3 h period.

The diminished F_{Ra} values in this 3 h period suggest an inhibition of autotrophic respiration shortly after light termination. Barbour et al. (2007) found that the respiration rate in bean leaves decreased rapidly within the first 20 min after light termination and either continued to slowly decrease with time or stabilize. Barbour et al. (2011) also found that the δ_R value of light-adapted leaves was enriched during the first minutes of dark respiration. These findings could help explain the changes in F_R observed in the soybean chamber. To our knowledge, there have been no studies concerning post-illumination changes in the carbon isotope ratio of respiration from C_4 plants. Several studies (Kirschbaum and Farquhar, 1987; Atkin et al., 1997; Shapiro et al., 2004; Hurry et al., 2005) have found that leaf respiration is inhibited in the presence of light, which our findings appear to contradict. However, leaf respiration was not directly measured in our study, meaning that inhibition may have occurred but was masked by diel variability in belowground plant and microbial respiration. Diminished F_R may have been influenced by the sudden termination of greenhouse lighting, indicating that this phenomenon was a product of greenhouse and growth chamber conditions and may not be observed in a field setting. These findings emphasize the need for further examination of above and below ground plant respiration and its isotope composition under natural field conditions.

3.3. Total conductance to CO_2

Although water loss was nearly equal for the planted and bare soil chambers shortly after watering, ET consistently remained higher in the planted chambers 24–72 h after each watering event (Fig. 4a). Values of ET exhibited a diel pattern in all chambers, reaching a maximum at 1200 h and a minimum at 0600 h (Fig. 4d). With E included in the calculation, the g_c signal exhibited rapid increases after watering events followed by gradual decreases until the next watering event (Fig. 4b). When E was excluded (Eq. 10), the g_c signal increased steadily due to the development of the vegetation (Fig. 4c). On Day 7 of the experiment, diel variation in g_c was minor,

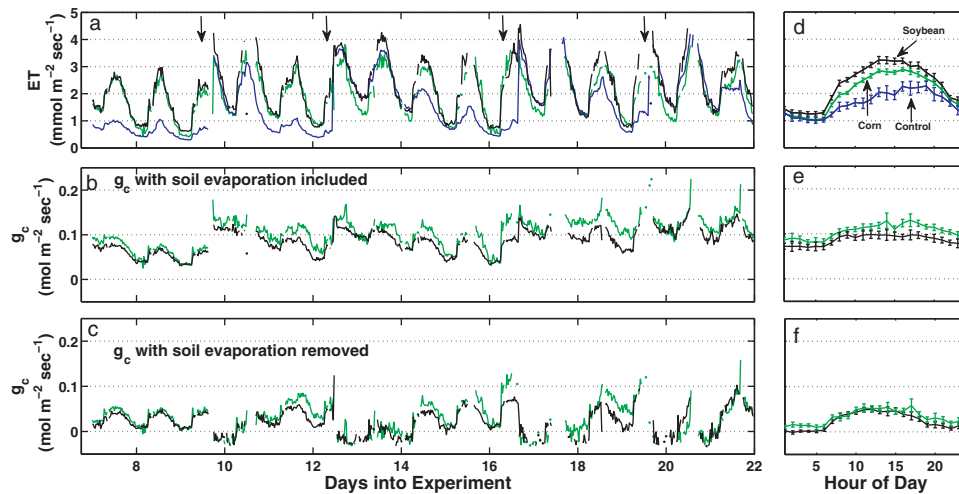


Fig. 4. Half hourly measurements of (a) Water vapor flux, (b) total conductance to CO_2 (g_c) with E included, and (c) g_c with E removed for the corn (green line), soybean (black line), bare soil (blue line) chambers. The black arrows in panel (a) indicate watering events. Panels (d), (e), and (f) represent the diel ensembles of panels (a), (b), and (c), respectively. (For interpretation of the references to color in this figure legend, the reader is referred to the web version of the article.)

reaching $0.05 \text{ mol m}^{-2} \text{ s}^{-1}$ at 1200 h and falling to $0.02 \text{ mol m}^{-2} \text{ s}^{-1}$ during the nighttime. By Day 20, midday g_c was $0.10 \text{ mol m}^{-2} \text{ s}^{-1}$ in both planted chambers with nighttime values near zero.

3.4. Evaluation of stable carbon isotope partitioning

Using stable carbon isotope techniques, F_N was partitioned into F_P and F_R for both the corn and soybean chambers (Fig. 5a and b). Diel ensembling was necessary to dampen noise in the measurement, specifically for g_c shortly after watering events and δ_N during the mid-morning and mid-evening transition periods when F_N was near zero. The estimated net photosynthetic flux increased sharply after greenhouse lighting was activated and reached -14.5 and $-10.7 \mu\text{mol m}^{-2} \text{ s}^{-1}$ at 1200 h in the corn and soybean chambers, respectively, before decreasing in the late afternoon and evening. Daytime respiration reached a maximum of $7.6 \mu\text{mol m}^{-2} \text{ s}^{-1}$ at 1200 h in the soybean chamber before gradually decreasing in the late afternoon and evening. In the corn chamber, daytime F_R reached $8.6 \mu\text{mol m}^{-2} \text{ s}^{-1}$ at about 1200 h before decreasing sharply from 1400 to 1800 h.

3.4.1. Influence of variability in g_c

As expected, the diel pattern of F_P was very similar to the diel pattern of g_c in both the corn and soybean chambers. Use of the bare soil control chamber effectively removed the soil evaporation signal from the planted chambers and allowed for a transpiration measurement with an improved signal to noise ratio and, as a result, a g_c measurement that better represented the true leaf conductance to CO_2 . A sensitivity analysis showed that estimates of F_P increased an average of 1.0 and $1.6 \mu\text{mol m}^{-2} \text{ s}^{-1}$ when g_c was increased by 10% in the soybean and corn chambers, respectively. When E was included in g_c , estimates of F_P were nearly doubled in both chambers and exhibited an unrealistic diel pattern, including strong nighttime uptake (not shown).

3.4.2. Variation in the bundle sheath leakage parameter ϕ

Variation in the CO_2 leakage factor ϕ also had a significant influence on calculated F_P values for C_4 partitioning. For this study, ϕ was optimized at 0.46, similar to the value of 0.42 assigned by Sun et al. (2010) but less than the 0.3 value assigned by Zhang et al. (2006). A sensitivity analysis showed that midday F_P increased by about $1.5 \mu\text{mol m}^{-2} \text{ s}^{-1}$ when ϕ was increased by

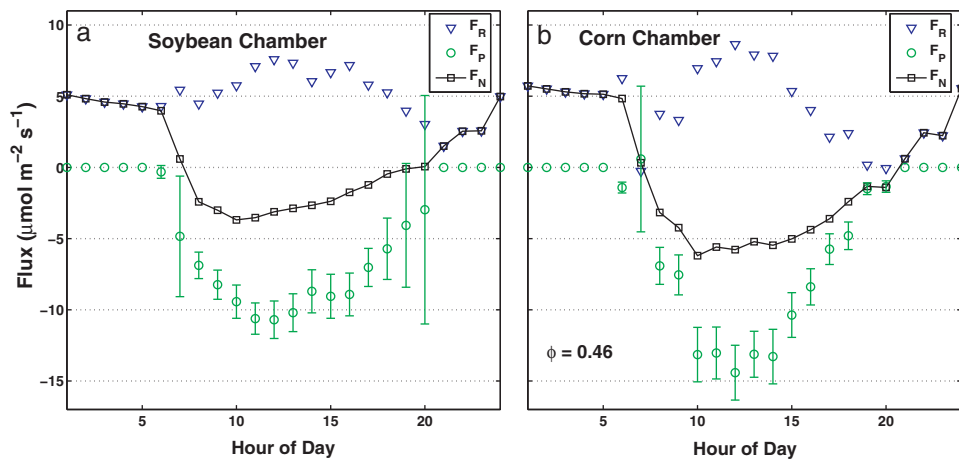


Fig. 5. Diel ensemble of F_N (black squares) partitioned into F_R (blue triangles) and F_P (green circles) from the corn and soybean chambers. Ensemble averages were created from the last 15 days of the experiment during peak growth. For C_4 partitioning, ϕ was assigned a value of 0.46. Nighttime values of F_P were forced to zero when $F_N = F_R$. Error bars represent the maximum probable error. See error propagation method described in Bevington and Robinson (2003) and Zhang et al. (2006). (For interpretation of the references to color in this figure legend, the reader is referred to the web version of the article.)

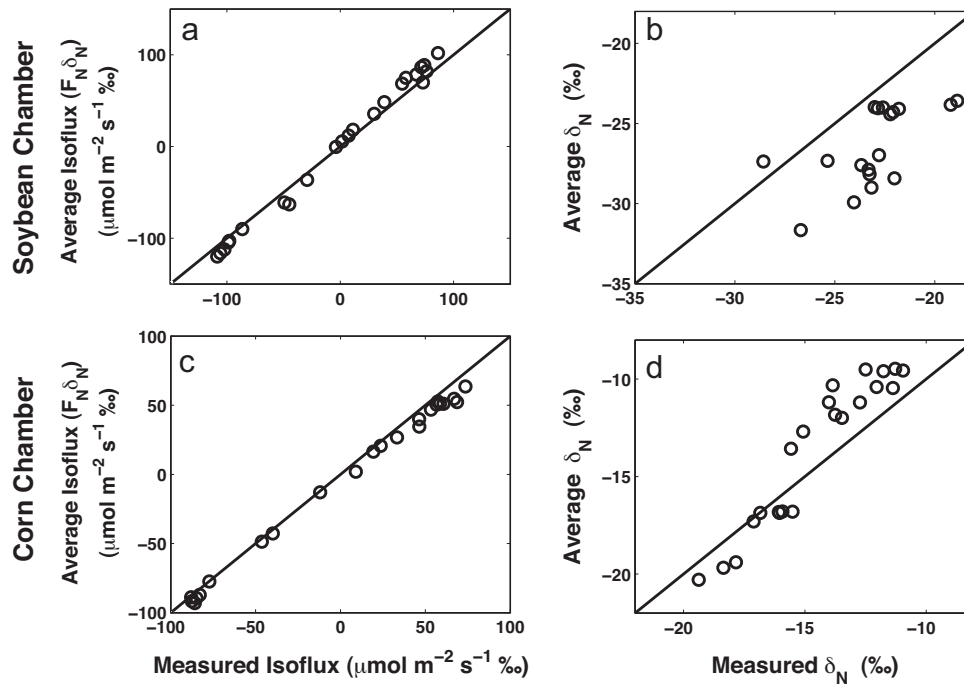


Fig. 6. One to one plots comparing modeled and measured values of the net CO_2 isoflux ($F_N \delta_N$), and δ_N for the corn (Panels a and b) and soybean (Panels d and e) chambers.

0.05. Despite the importance of ϕ in the C_4 partitioning method, few studies have examined the main factors controlling its variability (O’Leary, 1981; Sun et al., 2010). Given the sensitivity of the partitioning result to ϕ , further research is warranted in order to understand the processes controlling the CO_2 leakage factor.

Optimization of ϕ was tested by calculating both δ_N and the isoflux ($F_N \delta_N$) using the mass balance equation of $F_N \delta_N = F_p \delta_p + F_R \delta_R$. The δ_p term was assigned a value of -12‰ , equal to the average isotope composition of C_4 photosynthesis. The δ_R term was assigned a value of -17‰ , equal to the average nighttime measurement of δ_R observed during the experiment. For F_p , the values shown in Fig. 5b were used when ϕ was set at 0.46. The calculated δ_N and isoflux values were then compared to the measured values. Overall, the calculated isoflux agreed with the measured isoflux when ϕ was assigned a value of 0.46 ($r^2 = 0.99$, $n = 24$, Fig. 6c) while calculated δ_N showed a weaker correlation with the measured values ($r^2 = 0.45$, $n = 24$, Fig. 6d). Average daytime values of δ_N were consistently 2–3‰ higher than the measured values. More enriched average values of δ_N in the corn chamber could be due to an overestimation of F_p , which would have caused the sum of the respiratory and photosynthetic isofluxes to become less negative and lead to more enriched values of average δ_N . Also, more enriched average δ_N values could have been caused by either an average δ_p value that was too low or an average δ_R values that was too high.

A similar test was performed on the C_3 partitioning results, with δ_p equal to the average isotope composition of C_3 photosynthesis (-27‰) and δ_R equal to the average observed nighttime measurement of δ_R (-23‰). Testing of the C_3 partitioning results revealed that the modeled isoflux showed strong agreement with the measured values ($r^2 = 0.98$, $n = 24$, Fig. 6a). Measured values of δ_N , however, were consistently 3–5‰ more enriched than the average δ_N values (Fig. 6b). More depleted average δ_N values in the soybean chamber could have been due to an overestimation of F_p , which would have caused the sum of the photosynthetic and respiratory isofluxes to become more negative and, as a result, yielded more negative average δ_N values. For both planted

chambers, the potential overestimation of F_p may have been due to an overestimation of g_c (Eq. (4)).

3.4.3. Variability in δ_R

In the corn chamber, estimated values of F_p increased by an average of $5.8 \mu\text{mol m}^{-2} \text{s}^{-1}$ when δ_R was increased by 2‰ (with no diel variability) and decreased by $3.3 \mu\text{mol m}^{-2} \text{s}^{-1}$ when δ_R was decreased by 2‰. A similar influence was observed in the soybean chamber, with F_p increasing about $1.2 \mu\text{mol m}^{-2} \text{s}^{-1}$ when δ_R was increased by 2‰ and decreasing by about $1.1 \mu\text{mol m}^{-2} \text{s}^{-1}$ when δ_R was decreased by 2‰.

The incorporation of diel variability in δ_R also had a significant influence on F_N partitioning. A diel δ_R signal was simulated in the planted chambers by adding the variability about the mean observed in the bare soil control chamber (Fig. 3b) to average δ_R values of -17 and -23‰ for the corn and soybean chambers, respectively. Also, to account for diel variability in δ_R , nighttime F_p was re-adjusted to zero by re-optimizing ϕ to 0.48. Incorporation of the diel δ_R signal increased estimates of F_p by $6.5 \mu\text{mol m}^{-2} \text{s}^{-1}$ in the corn chamber, reaching $-21.0 \mu\text{mol m}^{-2} \text{s}^{-1}$ at 1200 h. In the soybean chamber, estimates of F_p were less affected by the incorporation of diel variability in δ_R , increasing by an average of $2.1 \mu\text{mol m}^{-2} \text{s}^{-1}$. In the corn chamber, a sensitivity analysis on δ_R with diel variability included showed an $8.1 \mu\text{mol m}^{-2} \text{s}^{-1}$ increase in estimated F_p when the diel δ_R signal was increased by 2‰ and a $5.5 \mu\text{mol m}^{-2} \text{s}^{-1}$ decrease when the diel δ_R signal was decreased by 2‰. In the soybean chamber, estimates of F_p were less sensitive to changes in δ_R with diel variability included, increasing or decreasing by about $1.2 \mu\text{mol m}^{-2} \text{s}^{-1}$ when δ_R was increased or decreased by 2‰, respectively. The strong influence of temporal variability in δ_R on C_3 and, in particular, C_4 partitioning emphasizes the importance of an accurate δ_R measurement and indicates the need for further research on the main factors controlling diel and seasonal variability in the isotope composition of autotrophic and heterotrophic respiration (Billmark and Griffis, 2009; Riveros-Iregui et al., 2011).

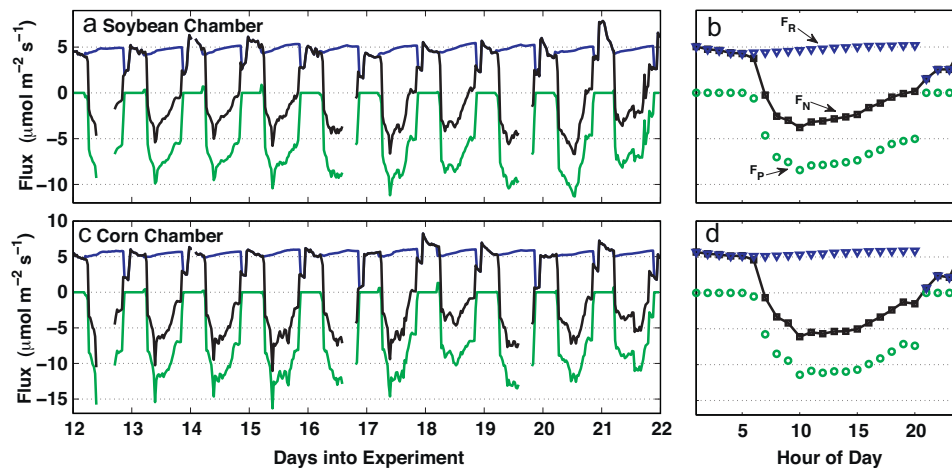


Fig. 7. Half hourly results of F_N (black squares) partitioned into F_R (blue diamonds) and F_P (green circles) for the corn and soybean chamber using a traditional temperature regression method. Panels on the right are the diel ensembles of the half-hourly results. Nighttime values of F_P were forced to zero when $F_N = F_R$. (For interpretation of the references to color in this figure legend, the reader is referred to the web version of the article.)

3.4.4. Isotope disequilibrium

For this study, the isotope disequilibrium, defined as the difference between δ_P and δ_R , was about 8‰ at the start of the greenhouse experiment for both planted chambers before gradually decreasing to about 4‰ at the end of the experiment. At the ecosystem-scale, Griffis et al. (2005) and Zhang et al. (2006) observed early growth disequilibrium values that were similar to those observed at the start of our greenhouse experiment but decreased to near zero during and shortly after peak growth. Several studies (Bowling et al., 2003b; Ogée et al., 2003; Zhang et al., 2006; Zobitz et al., 2007) have found that when the isotope disequilibrium approaches the resolution of the equipment, the isotope flux partitioning methodology is not reliable. In this study, the uncertainty in δ_N was approximately 0.5‰ which is significantly improved over previous studies using flux-gradient (Zhang et al., 2006), EC-flask (Bowling et al., 2001; Ogée et al., 2003), and EC-TDL (Billmark and Griffis, 2009) approaches. The relatively low noise on δ_N relative to the large isotope disequilibrium provided a more favorable partitioning result.

3.5. Partitioning with a traditional nighttime temperature regression model

Estimates of F_R were derived using the Q_{10} relationship of $F_R = F_{10} Q_{10}^{(T-10)/10}$. The relationship was then used to estimate daytime

respiration (Fig. 7). For our study, like all partitioning studies that utilize temperature-regression techniques, F_P was forced to zero when PAR was near zero. Estimates of F_P using the 5 cm temperature were about $2 \mu\text{mol m}^{-2} \text{s}^{-1}$ lower than estimates of F_P using the stable isotope partitioning method for both chambers (Fig. 8). The relatively low estimates of F_P were due to low Q_{10} values. Calculated Q_{10} values were 1.54 ($r^2 = 0.92$, $n = 10$) and 1.38 ($r^2 = 0.80$, $n = 10$) for the soybean and corn chambers, respectively, and similar to the values reported by Mahecha et al. (2010). For comparison, the Q_{10} value of F_R in the bare soil control chamber was 2.17 ($r^2 = 0.88$, $n = 10$). When air temperature was substituted for 5 cm soil temperature, Q_{10} values decreased to about 1.10 for both planted chambers with F_R exhibiting poor correlations to temperature ($r^2 < 0.1$). The weak correlations were due to an apparent lack of temperature sensitivity for nighttime values of F_R , which steadily decreased from 0000 to 0600 h while air temperature inside of the greenhouse was held constant during the same time period. Another period when F_R lacked temperature sensitivity was shortly after light termination when post-illumination processes appear to have inhibited autotrophic respiration. Our observations indicate a systematic difference in the daytime partitioned fluxes based on the isotope and temperature-regression methods. Estimates of F_P were symmetric with the diel F_N pattern when using the temperature-regression method. The isotope partitioning method, however, produced estimates of F_P that were symmetric with the

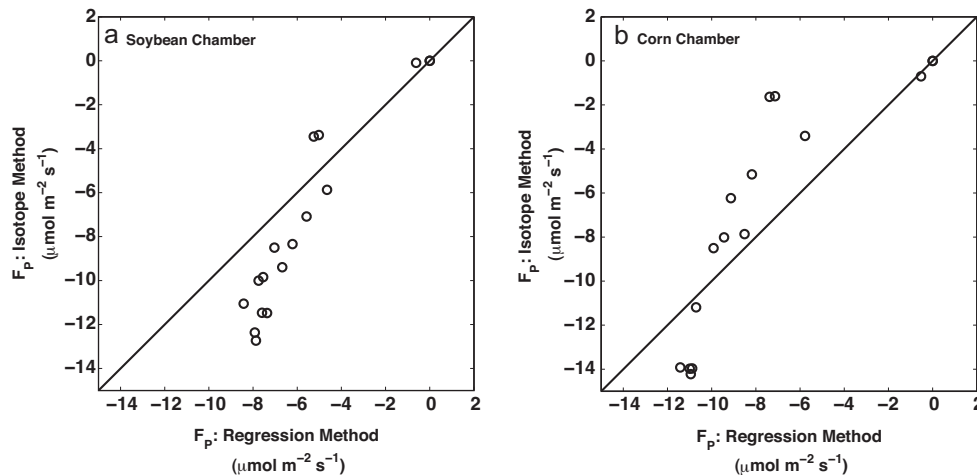


Fig. 8. Comparison of the diel ensembles of estimated F_P values from the isotope and temperature regression partitioning methods for the (a) soybean and (b) corn chambers, respectively.

diel g_c pattern. Also, daytime estimates of F_R were 2–3 $\mu\text{mol m}^{-2} \text{s}^{-1}$ higher using the isotope method than the temperature-regression method.

4. Conclusions

In this study we utilized an automated chamber system and a tunable diode laser under controlled environmental conditions to isolate potential limitations in the stable carbon isotope partitioning method. Results from this study indicate that:

- 1 Partitioning of net CO_2 exchange into its photosynthetic and respiratory components is improved when the variability in the isotope composition of respiration is accounted for and when the influence of soil evaporation is removed prior to calculating stomatal conductance.
- 2 Diurnal and short-term variation in the isotope composition of respiration had the greatest influence on partitioning results, causing photosynthetic uptake to nearly double. Surprisingly, variability in the isotope composition of respiration had a small influence on calculated photosynthesis values for soybean. Use of soil chambers may help estimate seasonal and diel variability in the isotope composition of respiration from below ground sources and may diminish uncertainty in the partitioned results.
- 3 Variation in the bundle sheath leakage factor caused significant changes to estimates of photosynthetic uptake in the corn chamber. While the optimization method used in this study appeared to be successful, the physiological explanation for why this optimized value was successful is unknown.
- 4 The carbon isotope and temperature-regression methods yielded very different diel patterns of F_P and F_R . This difference is partially attributed to the apparent lack of temperature sensitivity of processes that control autotrophic respiration. This was evident shortly after light termination when F_R decreased for reasons other than temperature. The diel F_P pattern was symmetric with the diel F_N pattern when using the temperature-regression method and symmetric with diel g_c pattern when using the isotope partitioning method. Also, daytime estimates of F_R were higher using the isotope method than the temperature-regression method.

Acknowledgments

We thank Matt Erickson and Bill Breiter for their technical assistance. We also thank Zoran Nestic and Dr. T.A. Black, Biometeorology and Soil Physics Group, University of British Columbia, for their help with the implementation of the automated chamber system. We acknowledge the very helpful comments and criticisms of two anonymous reviewers and the guest editor. We also thank Dr. David Bowling, University of Utah, for his detailed comments and criticisms of the revised manuscript. Funding for this research has been provided by the National Science Foundation, ATM-0546476 (TG) and the Office of Science (BER) U.S. Department of Energy, DE-FG02-06ER64316 (TG and JMB).

References

- Atkin, O., Westbeek, M., Cambridge, M., Lambers, H., Pons, T., 1997. Leaf respiration in the darkness: a comparison of slow- and fast-growing poa species. *Plant Physiol.* 113, 961–965.
- Baker, J.M., Griffis, T.J., 2005. Examining strategies to improve the carbon balance of corn/soybean agriculture using eddy covariance and mass balance techniques. *Agric. For. Meteorol.* 128, 163–177.
- Barbour, M., Hunt, J., Kodama, N., Laubach, J., McSeveny, T., Rogers, G., Tcherkez, G., Wingate, L., 2011. Rapid changes in $\delta^{13}\text{C}$ of ecosystem-respired CO_2 after sunset are consistent with transient ^{13}C enrichment of leaf respired CO_2 . *New Phytol.* 1–13.
- Barbour, M., McDowell, N., Tcherkez, G., Bickford, C., Hanson, D., 2007. A new measurement technique reveals rapid post-illumination changes in the carbon isotope composition of leaf-respired CO_2 . *Plant Cell Environ.* 30, 469–482.
- Bevington, P., Robinson, D., 2003. *Data Reduction and Error Analysis for the Physical Sciences*, 3rd edition. McGraw Hill.
- Billmark, K., Griffis, T., 2009. Influence of phenology and land management on biosphere–atmosphere isotopic CO_2 exchange. In: Noormets, A. (Ed.), *Phenology of Ecosystem Processes: Applications in Global Change Research*. Springer Science and Business Media, pp. 143–166.
- Bowling, D., Pataki, D., Ehleringer, J., 2003a. Critical evaluation of micrometeorological methods for measuring ecosystem-atmosphere isotopic exchange of CO_2 . *Agric. For. Meteorol.* 116, 159–179.
- Bowling, D., Sargent, S.D., Tanner, B.D., Ehleringer, J., 2003b. Tunable diode laser spectroscopy for stable isotope studies of ecosystem-atmosphere CO_2 exchange. *Agric. For. Meteorol.* 118, 1–19.
- Bowling, D., Tans, P., Monson, R., 2001. Partitioning net ecosystem carbon exchange with isotopic fluxes of CO_2 . *Global Change Biol.* 7, 127–145.
- Bowling, D.R., Pataki, D., Randerson, J., 2008. Carbon isotopes in terrestrial ecosystem pools and CO_2 fluxes. *New Phytol.* 178, 24–40.
- Bush, S., Pataki, D., Ehleringer, J., 2007. Sources of variation in $\delta^{13}\text{C}$ of fossil fuel emissions in Salt Lake City, USA. *Appl. Geochem.* 22 (4), 715–723.
- Cowan, I., Farquhar, G.D., 1977. Stomatal function in relation to leaf metabolism and environment. In: *Symposium of the Society for Experimental Biology*, vol. 31, pp. 471–505.
- Davidson, E.A., Belk, E., Boone, R.D., 1998. Soil water content and temperature as independent or confounded factors controlling soil respiration in a temperate mixed hardwood forest. *Global Change Biol.* 4, 217–227.
- Drewitt, G., Wagner-Riddle, C., Warland, J., 2009. Isotopic CO_2 measurements of soil respiration over conventional and no-till plots in fall and spring. *Agric. For. Meteorol.* 149, 614–622.
- Evans, J., Sharkey, T., Berry, J.A., Farquhar, G.D., 1986. Carbon isotope discrimination measured concurrently with gas exchange to investigate CO_2 diffusion in leaves of higher plants. *Aust. J. Plant Physiol.* 13 (2), 281–292.
- Falge, E., Baldocchi, D., Tenhunen, J., Aubinet, M., Bakwin, P., Berbigier, P., Bernhofer, C., Burba, G., Clement, R., Davis, K., Elbers, J., Goldstein, A., Grelle, A., Granier, A., Gundersson, J., Hollinger, D., Kowalski, A., Katul, G., Law, B., Malhi, Y., Meyers, T., Monson, R., Munger, J., Oechel, W., Paw, U., Pilegaard, K., Rannik, U., Rebmann, C., Suyker, A., Valentini, R., Wilson, K., Wofsy, S., 2002. Seasonality of ecosystem respiration and gross primary production as derived from fluxnet measurements. *Agric. For. Meteorol.* 113, 53–74.
- Farquhar, G., Ehleringer, J., Hubick, K., 1989. Carbon isotope discrimination and photosynthesis. *Annu. Rev. Plant Physiol. Plant Mol. Biol.* 40, 503–537.
- Farquhar, G.D., 1983. On the nature of carbon isotope discrimination in C_4 species. *Aust. J. Plant Physiol.* 10, 205–226.
- Farquhar, G.D., Sharkey, T., 1982. Stomatal conductance and photosynthesis. *Annu. Rev. Plant Physiol.* 33, 317–345.
- Fassbinder, J., Griffis, T., Baker, J., 2012. Interannual, seasonal, and diel variability in the carbon isotope composition of respiration in a C_3/C_4 agricultural ecosystem. *Agric. Forest Meteorol.* 153, 143–152.
- Gaumont-Guay, D., Black, T.A., Griffis, T.J., Barr, A.G., Jassal, R.S., Nestic, Z., 2006. Interpreting the dependence of soil respiration on soil temperature and water content in a boreal aspen stand. *Agric. For. Meteorol.* 140 (1–4), 220–235.
- Gessler, A., Tcherkez, G., Peuke, A., Ghashghaie, J., Farquhar, G.D., 2008. Experimental evidence for diel variations of the carbon isotope composition in leaf, stem and phloem sap organic matter in *Ricinus communis*. *Plant Cell Environ.* 31, 941–953.
- Ghashghaie, J., Duranceau, M., Badeck, F., Adeline, M.T., Cornic, G., Deléens, E., 2001. $\delta^{13}\text{C}$ of CO_2 respired in the dark in relation to $\delta^{13}\text{C}$ of leaf metabolites: comparison between *Nicotiana sylvestris* and *Helianthus annuus* under drought. *Plant Cell Environ.* 24, 505–515.
- Goulden, M., Munger, J., Fan, S.-M., Daube, B., Wofsy, S., 1996. Measurements of carbon sequestration by long-term eddy covariance: methods and a critical evaluation of accuracy. *Global Change Biol.* 2, 169–182.
- Griffis, T., Baker, J., Zhang, J., 2005. Seasonal dynamics and partitioning of isotopic CO_2 exchange in a C_3/C_4 managed ecosystem. *Agric. For. Meteorol.* 132 (1–2), 1–19.
- Griffis, T., Lee, X., Baker, J., Billmark, K., Schultz, N., Erickson, M., Zhang, X., Fassbinder, J., Xiao, W., Hu, N., 2011. Oxygen isotope composition of evapotranspiration and its relation to C_4 photosynthetic discrimination. *J. Geophys. Res.* 116, G01035.
- Griffis, T., Sargent, S., Baker, J., Lee, X., Tanner, B., Greene, J., Swiatek, E., Billmark, K., 2008. Direct measurement of biosphere–atmosphere isotopic CO_2 exchange using the eddy covariance technique. *J. Geophys. Res.* 113, D08304.
- Griffis, T.J., Baker, J.M., Sargent, S.D., Tanner, B.D., Zhang, J., 2004. Measuring field-scale isotopic CO_2 fluxes with tunable diode laser absorption spectroscopy and micrometeorological techniques. *Agric. For. Meteorol.* 124 (1–2), 15–29.
- Griffis, T.J., Black, T.A., Morgenstern, K., Barr, A.G., Nestic, Z., Drewitt, G.B., Gaumont-Guay, D., McCaughey, J.H., 2003. Ecophysiological controls on the carbon balances of three southern boreal forests. *Agric. For. Meteorol.* 117 (1–2), 53–71.
- Gu, L., Post, W., King, A., 2004. Fast labile carbon turnover obscures sensitivity of heterotrophic respiration from soil to temperature: a model analysis. *Global Biogeochem. Cycles* 18, 1–11.
- Hurry, V., Igamberdiev, A., Keerber, O., Parnik, T., Atkin, O., Zaragoza-Castells, J., Gardstrom, P., 2005. Respiration in Photosynthetic Cells: Gas Exchange Components, Interactions with Photorespiration and the Operation of Mitochondria in the Light. Springer.

- Keeling, C., 1958. The concentrations and isotopic abundances of atmospheric carbon dioxide in rural areas. *Geochim. Cosmochim. Acta* 13, 322–334.
- Kim, K., Lee, X., 2011. Transition of stable isotope ratios of leaf water under simulated dew formation. *Plant Cell Environ.* 34, 1790–1801.
- Kirschbaum, M., Farquhar, G., 1987. Investigation of the CO₂ dependence of quantum yield and respiration in *Eucalyptus pauciflora*. *Plant Physiol.* 83, 1032–1036.
- Klumpp, K., Schauffele, R., Lotscher, M., Lattanzi, F., Feneis, W., Schnyder, H., 2005. C-isotope composition of CO₂ respired by shoots and roots: fractionation during dark respiration? *Plant Cell Environ.* 28 (2), 241–250.
- Knohl, A., Buchmann, N., 2005. Partitioning the net CO₂ flux of a deciduous forest into respiration and assimilation using stable carbon isotopes. *Global Biogeochem. Cycles* 19, GB4008.
- Kodama, N., Barnard, R., Salmon, Y., Weston, C., Ferrio, J., Holst, J., Werner, R., Saurer, M., Rennenberg, H., Buchmann, N., Gessler, A., 2008. Temporal dynamics of the carbon isotope composition in a *Pinus sylvestris* stand: from newly assimilated organic carbon to respired carbon dioxide. *Physiol. Ecol.* 156, 737–750.
- Lasslop, G., Reichstein, M., Papale, D., Richardson, A., Arneeth, A., Barr, A., Stoy, P., Wohlfahrt, G., 2010. Separation of net ecosystem exchange into assimilation and respiration using a light response curve approach: critical issues and global evaluation. *Global Change Biol.* 16, 187–208.
- Lee, X., Wu, H., Sigler, J., Oishi, C., Siccama, T., 2004. Rapid and transient response of soil respiration to rain. *Global Change Biol.* 10, 1017–1026.
- Mahecha, M., Reichstein, M., Carvalhais, N., Lasslop, G., Lange, H., Seneviratne, S., Vargas, R., Ammann, C., Altaf Arain, M., Cescatti, A., Janssens, I., Migliavacca, M., Montagnani, L., Richardson, A., 2010. Global convergence in the temperature sensitivity of respiration at ecosystem level. *Science* 329, 838–840.
- Millard, P., Midwood, A., Hunt, J., Whitehead, D., Boutton, T., 2008. Partitioning soil surface CO₂ efflux into autotrophic and heterotrophic components, using natural gradients in soil $\delta^{13}\text{C}$ in an undisturbed savannah soil. *Soil Biol. Biochem.* 40, 1575–1582.
- Ogée, J., Peylin, P., Ciais, P., Bariac, T., Brunet, Y., Berbigier, P., Roche, C., Richard, P., Bardoux, G., Bonnefond, J.-M., 2003. Partitioning net ecosystem carbon exchange into net assimilation and respiration using ¹³CO₂ measurements: a cost-effective sampling strategy. *Global Biogeochem. Cycles* 17 (2), 1–18.
- O'Leary, M., 1981. Carbon isotope fractionation in plants. *Phytochemistry* 20, 553–567.
- Pataki, D., Ehleringer, J., Flanagan, L., Yakir, D., Bowling, D., Still, C., Buchmann, N., Kaplan, J., Berry, J.A., 2003a. The application and interpretation of keeling plots in terrestrial carbon cycle research. *Global Biogeochem. Cycles* 17, 1–15.
- Pataki, D.E., Bowling, D., Ehleringer, J., 2003b. Seasonal cycle of carbon dioxide and its isotopic composition in an urban atmosphere: anthropogenic and biogenic effects. *J. Geophys. Res.* 108, 4735.
- Reichstein, M., Falge, E., Baldocchi, D., Papale, D., Aubinet, M., Berbigier, P., Bernhofer, C., Buchmann, N., Gilmanov, T., Granier, T., Grünwald, T., Havránková, K., Ilvesniemi, H., Janous, D., Knohl, A., Laurila, T., Lohila, A., Loustau, D., Matteucci, G., Meyers, T., Miglietta, F., Ourcival, J., Pumpanen, J., Rambal, S., Rotenberg, E., Sanz, M., Tenhunen, J., Seufert, G., Vaccari, F., Vesala, T., Yakir, D., Valentini, R., 2005. On the separation of net ecosystem exchange into assimilation and ecosystem respiration: review and improved algorithm. *Global Change Biol.* 11, 1424–1439.
- Riveros-Iregui, D., Hu, J., Burns, S., Bowling, D., Monson, R., 2011. An interannual assessment of the relationship between the stable carbon isotopic composition of ecosystem respiration and climate in a high elevation subalpine forest. *J. Geophys. Res.* 116, G02005.
- Rochette, P., Flanagan, L., Gregorich, E., 1999. Separating soil respiration into plant and soil components using analyses of the natural abundance of carbon-13. *Soil Sci. Soc. Am. J.* 63 (5), 1207–1213.
- Rustad, L.E., Huntington, T.G., Boone, R.D., 2000. Controls on soil respiration: implications for climate change. *Biogeochemistry* 48 (1), 1–6.
- Shapiro, J., Griffin, K., Lewis, J., Tissue, D., 2004. Response of *Xanthium strumarium* leaf respiration in the light to elevated CO₂ concentration, nitrogen availability and temperature. *New Phytol.* 162, 377–386.
- Sun, W., Resco, V., Williams, D., 2010. Nocturnal and seasonal patterns of carbon isotope composition of leaf dark-respired carbon dioxide differ among dominant species in a semiarid savanna. *Oecologia* 164, 297–310.
- Susfalk, R., Cheng, W., Johnson, D., Walker, R., Verburg, P., Fu, S., 2002. Lateral diffusion and atmospheric CO₂ mixing compromise estimates of rhizosphere respiration in a forest soil. *Can. J. For. Res.* 32, 1005–1015.
- Taiz, L., Zeiger, E., 2002. *Plant Physiology*, 3rd edition. Sinauer Associates Inc., Sunderland, MA, p. 690.
- Wagner, S., Reicosky, D., Alessi, R., 1997. Regression models for calculating gas fluxes measured with a closed chamber. *Agron. J.* 89, 279–284.
- Yakir, D., Wang, X., 1996. Fluxes of CO₂ and water between terrestrial vegetation and the atmosphere estimated from isotope measurements. *Nature* 380, 515–517.
- Zhang, J., Griffis, T., Baker, J., 2006. Using continuous stable isotope measurements to partition net ecosystem CO₂ exchange. *Plant Cell Environ.* 29 (4), 483–496.
- Zobitz, J., Burns, S., Ogée, J., Reichstein, M., Bowling, D., 2007. Partitioning net ecosystem exchange of CO₂: a comparison of a Bayesian/isotope approach to environmental regression methods. *J. Geophys. Res.* 112, G03013.
- Zobitz, J., Burns, S., Reichstein, M., Bowling, D., 2008. Partitioning net ecosystem carbon exchange and the carbon isotopic disequilibrium in a subalpine forest. *Global Change Biol.* 14, 1785–1800.